

# Particle Morphology in Artificial Composite Polymer Latex Systems

YI-CHERNG CHEN, VICTORIA DIMONIE, and MOHAMED S. EL-AASSER\*

Emulsion Polymers Institute, Center for Polymer Science and Engineering and Department of Chemical Engineering, Lehigh University, Bethlehem, Pennsylvania 18015

## SYNOPSIS

Artificial composite latex particles were prepared by direct emulsification of a toluene solution of a blend of polystyrene (PS) and poly(methyl methacrylate) (PMMA). The morphology of the composite particles from the higher molecular weight polymers showed polystyrene particles partially encapsulated by PMMA on the surface. On the other hand, for the lower molecular weight polymers, the reverse morphology was observed. The morphologies of the artificial composite latex particles swollen with solvent were examined when kept under agitation. The degree of phase separation between the two polymers in the composite particles was found to be affected by agitation to different extent, depending on the viscosity of polymer phases, the interfacial tension, and degree of mixing at interface between the two polymers. Extended agitation of the composite latex particles of high molecular weight polymers resulted in mixed morphologies that included individual PS and PMMA particles along with the original morphology of the composite particles. On the other hand, composite latex particles with the lower molecular weight polymers resisted complete phase separation due to lower interfacial tension and better mixing at the interface between the two polymers.

## INTRODUCTION

Control of composite latex particle morphology is important for many applications. Elucidation of the morphology of composite particle and possibility of controlling it were the goals of many studies published in recent years. Recently, it was demonstrated<sup>1,2</sup> that thermodynamic and kinetic factors dictate the particle morphology. The thermodynamic factors determine the stability of the ultimate particle morphology according to the minimum surface free energy change principle. Polymer-water and polymer-polymer interfacial tensions have been proved as key parameters deciding the thermodynamically preferred morphology. However, the kinetic factors such as viscosity of polymerization loci and the mode of second-stage monomer addition determine the ease with which

such a thermodynamically preferred morphology can be achieved.<sup>2-5</sup>

In the present work we studied the morphologies of artificial composite latex systems prepared by the direct emulsification method. This method involves preparation of a solution of a blend of two polymers in a mutual solvent, creation of an oil-in-water emulsion via homogenization, and then removal of the solvent by evaporation. The required polymer concentration in the oil phase is lower than the critical polymer concentration for demixing in order to start with a homogeneous polymer mixture in the solvent phase. This approach represents in essence the preparation of artificial latex<sup>6,7</sup> and is physically similar to the production of composite latexes via seeded emulsion polymerization when the chosen solvent happens to be the second-stage monomer. The main difference in particle preparation between the two methods is the lack of an initiator, which can trigger some grafting reaction between the second-stage polymer and the first-stage polymer in the seeded emulsion polymerization approach.

\* To whom correspondence should be addressed.

## THERMODYNAMIC BACKGROUND

The thermodynamic analysis that will be considered for determining the latex particle morphology is based on the approach presented 20 years ago by Torza and Mason.<sup>8</sup> They studied the interfacial behavior of systems containing three mutually immiscible liquids. In this case the thermodynamics of the system was influential since the liquid phase was highly mobile, i.e., low viscosity. They examined the conditions necessary for a coacervate droplet (liquid 3) to engulf an initial droplet (liquid 1) when both are immersed in a continuous phase (liquid 2) by the spreading coefficient,  $S$ , which is defined as

$$S_i = \gamma_{jk} - (\gamma_{ij} + \gamma_{ik}) \quad (1)$$

By assuming that the interfacial tension of liquid 1 against liquid 2 ( $\gamma_{12}$ ) is greater than that of liquid 3 against liquid 2 ( $\gamma_{23}$ ), only three possible sets of values for  $S$  exist. These correspond to the three different equilibrium configurations: complete engulfing (core-shell), partial engulfing (hemisphere),

and nonengulfing (individual particle). Complete engulfing occurs only if  $S_3 > 0$ ,  $S_2 < 0$ , and  $S_1 < 0$ . On the other hand, when  $S_2 < 0$ ,  $S_3 < 0$ , and  $S_1 < 0$ , partial engulfing was preferred. Torza and Mason demonstrated the general validity of their approach by making a number of interfacial tension measurements, calculating values of  $S$ , and then observing what occurred in the actual three-phase system. In most cases prediction of engulfing based on  $S$  were satisfactory. This approach should be broadly applicable in determining when engulfing will occur in various encapsulation systems. Recently, Sundberg et al.,<sup>9</sup> by applying Torza and Mason's approach, presented a thermodynamic analysis of the morphology of polymer encapsulating a relatively large size oil droplet in the micrometer range. Their analysis revealed that the interfacial tension of each phase is the key factor governing the type of microcapsules formed (core-shell, hemispheres, or individual particles).

In our previous work<sup>1,2</sup> a thermodynamic analysis similar to that presented by Sundberg et al.<sup>9</sup> and a mathematical model were derived to describe the

**Table I Free Energy Changes for Various Morphological Structures of Latex Particles Dispersed in Water<sup>a</sup>**

Case	$\Delta\psi$ (Surface Energy/Area)	Equation No.
A (core-shell)	$F[\gamma_{12}(V_r + 1)^{-2/3} + \gamma_{2w}] - \gamma_{1w}Y$	(3)
A' (inverted core-shell)	$F[\gamma_{12}(V_r^{-1} + 1)^{-2/3} + \gamma_{1w}] - \gamma_{1w}Y$	(4)
C (hemisphere 1)	$(F/2)[(V_r + 1)^{-2/3}\gamma_{1w}(1 + \cos \theta) + (V_r + 1)^{-2/3}(1 - \cos \theta)\gamma_{12} + (R_2/R)^2(1 + \cos \theta)\gamma_{2w}] - \gamma_{1w}Y$	(5)
	$\left(\frac{R_2}{R}\right)^3 = \frac{1 - (V_r + 1)^{-1}\{1 - (\frac{1}{8})(1 - \cos \theta)[3 \sin^2 \theta + (1 - \cos \theta)^2]\}}{1 - (\frac{1}{8})(1 - \cos \theta)[3 \sin^2 \theta + (1 - \cos \theta)^2]}$	(6)
	$\frac{R_2}{R} = \frac{(V_r + 1)^{-1/3} \sin \theta}{\sin \theta'}$	(7)
C' (hemisphere 2)	$(F/2)[(R_1/R)^2(1 + \cos \theta)\gamma_{1w} + \gamma_{12}(1 - \cos \theta)(V_r^{-1} + 1)^{-2/3} + (V_r^{-1} + 1)^{-2/3}(1 + \cos \theta)\gamma_{2w}] - \gamma_{1w}Y$	(8)
	$\left(\frac{R_1}{R}\right)^3 = \frac{1 - (V_r^{-1} + 1)\{1 - (\frac{1}{8})(1 - \cos \theta)[3 \sin^2 \theta + (1 - \cos \theta)^2]\}}{1 - (\frac{1}{8})(1 - \cos \theta)[3 \sin^2 \theta + (1 - \cos \theta)^2]}$	(9)
	$\frac{R_1}{R} = \frac{(V_r^{-1} + 1)^{-1/3} \sin \theta}{\sin \theta'}$	(10)
D (individual particles)	$F(\gamma_{1w} + \gamma_{2w}V_r^{2/3})(V_r + 1)^{-2/3} - \gamma_{1w}Y$	(11)

<sup>a</sup>  $Y = K(V_f + 1)^{-2/3}$ ,  $K = (1 + W_r d_1/d_{2m})^{2/3}$ ,  $V_f = W_r d_1/d_2$  and  $F = [Y^{3/2} + (1 - d_2/d_{2m})X/(1 + 1/V_f)]^{2/3}$ ,  $d_1$ ,  $d_2$ , and  $d_{2m}$  are the densities of polymer 1, polymer 2, and monomer 2, respectively.  $W_r$  is weight ratio of total monomer 2 to polymer 1.  $X$  is polymerization conversion.  $R_1$ ,  $R_2$ , and  $R$  are the radii of polymer phase 1, polymer phase 2, and the overall composite particle, respectively.  $\theta$  or  $\theta'$  (see Fig. 1), are the angles between the line that connects the two centers of the hemispheres and the other line that connects the centers and the three-phase point.  $\gamma_{12}$ ,  $\gamma_{1w}$ , and  $\gamma_{2w}$  are interfacial tensions between the two polymer phases; polymer phase 1 and water (containing surfactant, if present), and polymer phase 2 and water (containing surfactant, if present), respectively. A polymer phase is defined as polymer 1 or 2 dissolved in MMA monomer.  $V_r$  is the volume ratio of polymer phase 2 to polymer phase 1.

free energy changes (see Table I) corresponding to various composite latex particle morphologies shown in Figure 1. The methodology is first to consider the free energy changes for the following hypothetical pathways. The initial state consists of a polymer phase 1 (seed particle of polymer 1 swollen by second-stage monomer, i.e., monomer 2) suspended in water containing some surfactant. The final state is one of the morphologies shown in Figure 1. The  $\theta$  and  $\theta'$  shown in the hemisphere 1 and 2 cases are angles between the line that connects the two centers of the hemispheres and the other line that connects the centers and the three-phase point. The  $\theta$  angle will be used to describe the degree of phase separation of the composite particle morphology or magnitude of the surface area of core polymer phase covered by shell polymer phase. The increase of  $\theta$  angle will decrease the degree of phase separation (i.e., the increase of interface area between two polymer phases). The core-shell morphology (case A or A'') is the case that has  $\theta$  equal to  $180^\circ$ . The individual particle morphology (case D) has  $\theta$  equal to  $0^\circ$ . The only contribution to the free energy change for this pathway is the creation of new in-

terfaces and changes in the corresponding interfacial tensions. For latex particles dispersed in a continuous water phase, those interfaces include polymer phase 1/water, polymer phase 2/water, and polymer phase 1/polymer phase 2. The polymer phase 2 is polymer 2 (formed as a result of the polymerization of monomer 2 in the presence of polymer 1) swollen by its own monomer. The total concentration of monomer 2 is dependent on conversion. The monomer distribution between polymer 1 and 2 is assumed to be proportional to the volume fraction of each polymer. The total free energy change for all types of configurations shown in Figure 1 can be expressed as

$$\Delta G = \sum \gamma_{ij} A_{ij} - \gamma_{1w} A'_0 \quad (2)$$

where  $\gamma_{ij}$  is the interfacial tension between  $i$  and  $j$  and  $A_{ij}$  is the corresponding interfacial area. Each of the morphologies shown in Figure 1 has different combinations of  $\gamma_{ij} A_{ij}$ , depending on their geometric feature:  $\gamma_{1w}$  is the interfacial tension of the seed particles of polymer 1 swollen with monomer 2 suspended in water (containing surfactant, if present) and  $A'_0$  is its interfacial area. The equations describing the free energy change for each case shown in Figure 1 are summarized in Table I. The thermodynamically preferred morphology will be the one that has the minimum interfacial free energy change. Calculation of the free energy change by the equations listed in Table I involves a trial-and-error solution method. A FORTRAN77 computer program was prepared for this purpose. This approach is feasible if all of the  $\gamma_{ij}$  can be measured independently.

In our previous publications we demonstrated the applicability of this approach to predict the particle morphology in seeded emulsion polymerization for the preparation of composite of polystyrene (PS) and poly(methyl methacrylate (PMMA) latex systems and investigated the influence of monomer-polymer ratio,<sup>2</sup> surfactant types,<sup>10</sup> and initiator types.<sup>1</sup> The preceding thermodynamic analysis was extended for the case of preparation of artificial composite latex particles by direct emulsification of a solution of a blend of two polymers. In the present case the initial state is spherical droplets of toluene solution of the two polymers suspended in aqueous solution of the appropriate surfactant. Evaporation of the solvent will result in increasing the polymer concentration inside the droplets above the demixing level with the result of phase separation of the two polymers. The extent of phase separation and the final latex particle morphology will be dictated by

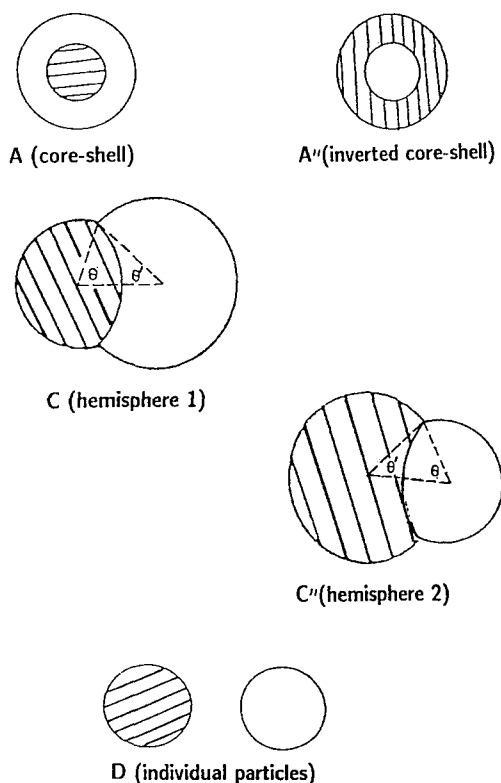


**Figure 1** Various morphological structures of particles dispersed in water: hatched area: polymer 1; open area: polymer 2.

the balance of the three interfacial tensions, polymer phase 1 against aqueous solution of surfactant; polymer phase 2 against aqueous solution of surfactant, and polymer phase 1 and polymer phase 2. The polymer phase refers to a solution of the appropriate polymer in a solvent.

## EXPERIMENTAL

### Materials

Methyl methacrylate monomer (Rohm and Haas Co.) was washed with 10% aqueous sodium hydroxide solution, followed by water, dried overnight (at 5°C) with anhydrous sodium sulfate (100 g/L) and vacuum distilled under dry nitrogen to remove the inhibitor. Styrene monomer (Polyscience) was washed with 10% aqueous sodium hydroxide solution, followed by water, dried overnight (at 5°C) with anhydrous sodium sulfate (100 g/L) and passed through an activated aluminum oxide column to remove the inhibitor. Azobisisobutyronitrile initiator (Vazo 64, du Pont Co.) was recrystallized twice from ethanol and then dried at room temperature in a vacuum oven. All other materials were used as received including potassium persulfate initiator ( $K_2S_2O_8$ , Fisher Scientific Co.), sodium bicarbonate buffer (Fisher Scientific Co.), Pluronic F-108 (polyethylene oxide-propylene oxide, 80% polyoxyethylene, BASF/Wyandotte), 1-butanol (ACS grade, Fisher Scientific Co.), and methanol (American Burdick & Jackson), cyclohexane (ACS grade, Fisher Scientific Co.), and toluene (ACS grade, Fisher Scientific Co.). Double-distilled deionized (DDI) water was used in the preparation of aqueous solutions.

### Polymer Preparation

Table II shows the recipes used in the preparation of two polystyrene (PS-1s and PS-2s) and

**Table II Solution Polymerization Recipes for PS and PMMA**

	PS (g)	PMMA (g)
Cyclohexane	30	
Styrene	10	
AIBN	0.011	0.022
Methyl methacrylate		10
Toluene		30

**Table III Recipe Used in the Direct Emulsification of PS and PMMA Polymer Solution**

Compons	Weight (g)
DDI water	75
Pluronic F-108	0.28
Polymer solution	
Toluene	23
Polystyrene	1
Poly(methyl methacrylate)	1

two poly(methyl methacrylate) (PMMA-1s and PMMA-2s) samples by solution polymerization. Batch solution polymerizations were carried out in rotating bottles at different temperatures for two days. PS-1s and PMMA-1s polymers were polymerized at 70°C. PS-2s and PMMA-2s were polymerized at 75°C using AIBN initiator. The polymers were then precipitated by adding their solutions to methanol and stirring for a period of time. The precipitated polymers were then filtered and dried in an oven at 40°C.

### Viscosity-Average Molecular Weight $M_v$

The viscosity-average molecular weight  $M_v$ , was measured using the Ubbelohde dilution viscometer at 25°C. Toluene and acetone were employed as solvents for PS and PMMA, respectively. The relationship between viscosity-average molecular weight and intrinsic viscosity is given by the following equation<sup>11</sup>:

$$[\eta] = 1.7 \times 10^{-4} [M]^{0.69} \quad (\text{for PS-toluene}) \quad (12)$$

$$[\eta] = 0.75 \times 10^{-4} [M]^{0.7} \quad (\text{for PMMA-acetone}) \quad (13)$$

### Direct Emulsification

The artificial composite latexes used in our morphology studies were prepared by direct emulsification method. Two artificial composite latex systems, PS-1s/PMMA-1s and PS-2s/PMMA-2s, were prepared using the corresponding polymers prepared by solution polymerization. The standard recipe is given in Table III. The artificial composite latex was prepared using Pluronic F-108 surfactant, 0.37% by weight based on water. An Omni Mixer (Sorvall) was used to mix the polymer solution in toluene and the water phase containing Pluronic F-108 surfactant at room temperature. The Omni

Mixer was operated at 16,000 rpm for 10 min. The preemulsion was then subjected to ultrasonification for 2 min at power 7, duty cycle = 80%. The stability of the resultant emulsion was evaluated by shelf storage life by storing a fraction of the emulsion in a test tube for one month at room temperature. The shelf storage tests showed that the resultant polymer emulsions creamed but were redispersible upon shaking. The remaining resultant polymer emulsion was vacuum stripped at 40°C to remove the solvent (toluene), giving the artificial latex. The extent of toluene removed was detected by gas chromatography using methanol as diluent and butanol as external standard. After the toluene was removed, DDI water was added into the artificial latex to keep the polymer-water ratio the same as that in recipe.

### Morphology Observation for the PS-1s/PMMA-1s Latex System

The morphology of the artificial composite latex particles was examined by using the transmission electron microscopy (TEM) after preferential staining. For this purpose a small sample of the artificial composite PS-1s/PMMA-1s latex particles containing a known amount of toluene was first put on TEM grids and almost instantaneously dried in a high-vacuum chamber at room temperature. The latex particles were then subjected to preferential staining of the polystyrene domains with RuO<sub>4</sub> vapor and negative staining with phosphotungstic acid (PTA) to better delineate the particle edges.<sup>12</sup> In parallel, a sample of the artificial composite latex containing the same known amount of toluene was stored and stirred by tumbling at 30 rpm for various periods of time. The morphologies were observed again by TEM under identical conditions to those applied to the original unstored sample. The morphology observation was repeated at different storage time periods.

### Morphology Observation for the PS-2s/PMMA-2s Latex System

To observe the morphology of the PS-2s/PMMA-2s composite latex particles, several samples were prepared as described in the following discussion.

*Sample 1t.* The artificial composite latex particles after removing all the toluene was stirred by tumbling at 30 rpm for 30 days at room temperature.

*Sample 2.* The artificial composite latex particles after removing all the toluene was reswollen by adding toluene into the latex and then stored undisturbed for 30 days at room temperature. The poly-

mer concentration in the toluene-swollen latex particles was 0.35 g/cm<sup>3</sup>.

*Sample 2t.* The artificial composite latex particles after removing all the toluene was reswollen again by adding toluene and then stirred by tumbling at 30 rpm for 30 days at room temperature. The polymer concentration in the toluene-swollen latex particles was 0.35 g/cm<sup>3</sup>.

*Sample 3.* The artificial composite latex after removing all the toluene was re-swollen by adding cyclohexane, which is a solvent for PS and a nonsolvent for PMMA, and then stored undisturbed for 30 days at room temperature. The polymer concentration in the cyclohexane-swollen latex particles was 0.35 g/cm<sup>3</sup>.

*Sample 3t.* The artificial composite latex after removing all the toluene was re-swollen by adding cyclohexane and then kept under tumbling at 30 rpm for 30 days at room temperature. The polymer concentration in the cyclohexane-swollen latex particles was 0.35 g/cm<sup>3</sup>.

Each sample was first put on a TEM grid and almost instantaneously dried in a high-vacuum chamber at room temperature. The morphologies were then examined by TEM after preferential staining of polystyrene domains with RuO<sub>4</sub> vapor and negative staining with PTA.

### Polymer-Water Interfacial Tension Measurement

The drop-volume interfacial tension measurements<sup>13</sup> were done at room temperature for the following three systems: (1) The mutually saturated toluene-water interface. (2) System 1 with the addition of a small amount of nonionic surfactant to the aqueous phase. For this purpose Pluronic F-108, in concentration of 0.37% by weight based on water, was used in order to simulate the prevailing conditions during the preparation of artificial composite latex. (3) System 2, where a polymer PS (or PMMA) was added to the toluene phase in increased concentrations while keeping the surfactant concentration in the aqueous phase unchanged. For each sample at least three interfacial tension measurements were done and the average was calculated.

## RESULTS AND DISCUSSION

### Viscosity-Average Molecular Weight $M_v$

Table IV lists the viscosity-average molecular weights ( $M_v$ ) of PS-1s, PS-2s, PMMA-1s, and PMMA-2s polymers. The data indicate that PS-1s

**Table IV** Viscosity-Average Molecular Weights of PS-1s, PMMA-1s, PS-2s, and PMMA-2s

	Sample	$M_v$
Sample 1	PS-1s	$0.94 \times 10^5$
	PMMA-1s	$1.12 \times 10^5$
Sample 2	PS-2s	$0.84 \times 10^5$
	PMMA-2s	$0.95 \times 10^5$

and PMMA-1s polymers prepared at lower polymerization temperature (70°C) have higher molecular weights than PS-2s and PMMA-2s prepared at 75°C, respectively.

### Interfacial Tension of Polymer–Water Interface

The experimental interfacial tension results for the toluene solutions of each one of the four polymers (PS-1s, PMMA-1s, PS-2s, and PMMA-2s) at different concentrations against aqueous solutions of the surfactant (0.37 wt % Pluronic F-108) are given in Figure 2. The interfacial tension data given in Figure 2 represent an average of all measurements, with a precision of  $\pm 0.02$  dyn/cm. The results show that the interfacial tension initially decreases with increasing polymer concentration, followed by an equilibrium region, in which the interfacial tension stays constant with increasing the polymer concentration. This is because the polar components of polymer (e.g., polymer chains with CN end groups) are more surface active than the nonionic surfac-

tants and contribute to the decrease in interfacial tension. It seems that the CN-containing polymer chains displace the surfactant at the interface thus increasing the polarity of interface between polymer (in toluene) and water, until the polarity reaches a certain equilibrium point depending on the amount and nature of the polar components of the polymer. The PS-2s and PMMA-2s polymers exhibited lower equilibrium polymer phase–water interfacial tensions than PS-1s and PMMA-1s polymers, respectively, due to their lower molecular weights and therefore, larger number of surface polar end groups from the initiator.<sup>14</sup> The PS-2s polymer exhibited a lower equilibrium interfacial tension ( $7.29 \pm 0.02$  dyn/cm) than PMMA-2s polymer ( $7.53 \pm 0.02$  dyn/cm). However, the PMMA-1s polymer showed a lower equilibrium interfacial tension ( $8.23 \pm 0.02$  dyn/cm) than PS-1s polymer ( $8.82 \pm 0.02$  dyn/cm). Therefore, based on thermodynamic consideration, when the composite latex particles (PS-2s/PMMA-2s) are formed, it is expected that the PS domain should encapsulate the PMMA domains. This type of encapsulation is the reverse to that of PS-1s/PMMA-1s composite latex system. This prediction was verified experimentally in the following sections.

### Morphology Observation for the PS-1s/PMMA-1s Latex System

Upon the removal of toluene from the resultant polymer emulsion, the polymer concentration in the oil phase (toluene-swollen latex particles) is increased. When the polymer concentration in the

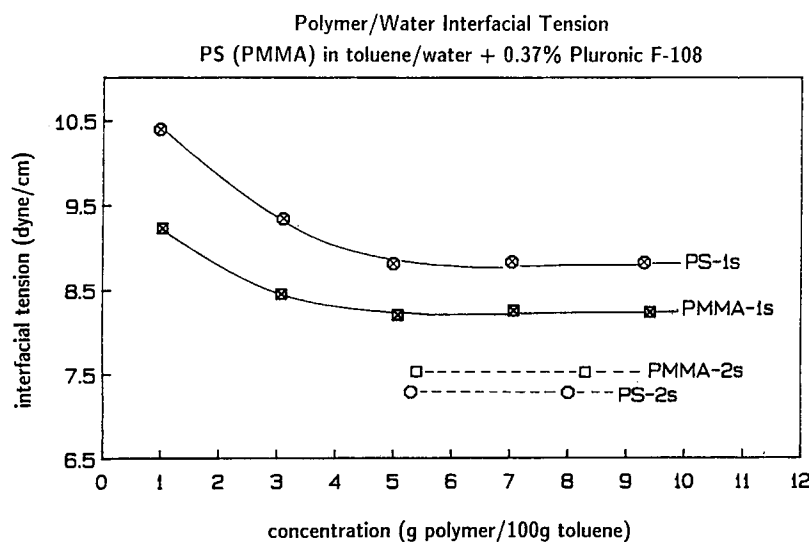


**Figure 2** Interfacial tensions at 25°C for PS-1s in toluene–water, PMMA-1s in toluene–water, PS-2s in toluene–water, and PMMA-2s in toluene–water systems.

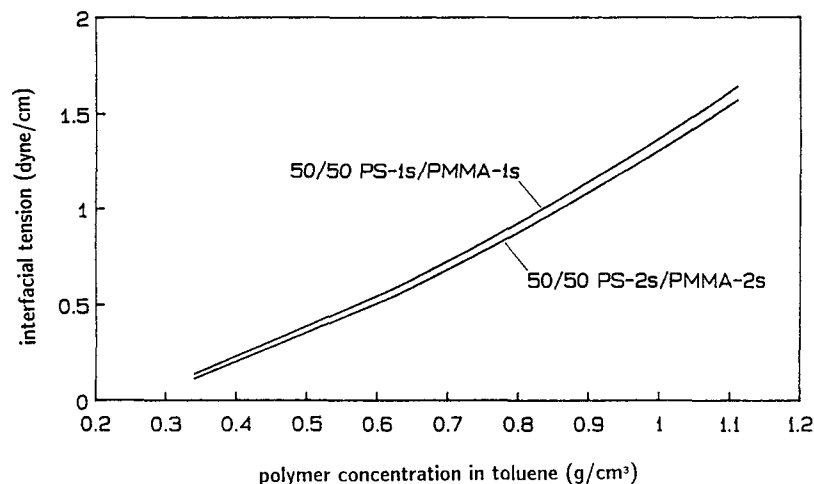


**Figure 3** The calculated interfacial tensions of 50/50 weight ratio of polymer 1/polymer 2 systems of PS-1s/PMMA-1s and PS-2s/PMMA-2s as a function of polymer concentration in toluene.

toluene-swollen latex particles becomes higher than the critical polymer concentration of demixing, further increase in polymer concentration results in an increase of polymer phase 1/polymer phase 2 in-

terfacial tension (see Fig. 3), and therefore separation of the two polymer phases. Figure 3 shows the calculated interfacial tensions between the two polymers as a function of polymer concentration in

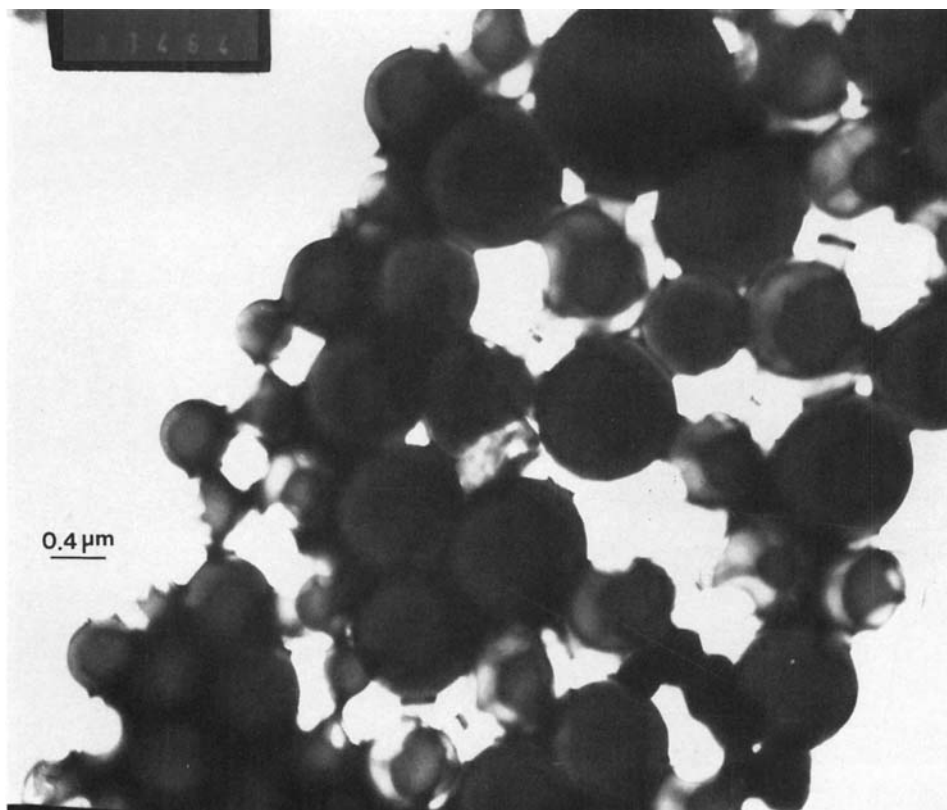


**Figure 4** TEM of PS-1s/PMMA-1s artificial composite latex particle morphology at  $0.6 \text{ g/cm}^3$  polymer concentration in toluene-swollen latex particles.

toluene for PS-1s/PMMA-1s and PS-2s/PMMA-2s systems at 50/50 polymer 1/polymer 2 weight ratio. These calculated polymer–polymer interfacial tensions were based on the work of Broseta et al.,<sup>15</sup> according to the approach outlined previously.<sup>1</sup>

The development of polymer phase separation and particle morphology in artificial composite particle involves the migration or diffusion of polymer chains, which is highly dependent on the local viscosity inside the particles, a kinetic factor. Figure 4 shows the particle morphology of PS-1s/PMMA-1s artificial composite latex at 0.6 g/cm<sup>3</sup> polymer concentration in the toluene-swollen latex particles. Since the time frame for removing the toluene to reach this concentration was not long enough to complete the phase separation of PS and PMMA polymers, the predicted particle morphology with PMMA lighter region encapsulating the PS dark region cannot be observed clearly. This type of encapsulation is imposed by the lower interfacial tension of PMMA polymer in toluene against aqueous phase than that of PS polymer (see Fig. 2).

Figure 5 shows the particle morphology of PS-

1s/PMMA-1s artificial composite latex, at 0.6 g/cm<sup>3</sup> polymer concentration in the toluene-swollen latex particles, after tumbling the latex for one week. Although the time frame to complete the separation of PS and PMMA polymer phases inside the particles was extended by storing and tumbling these composite particles, it is interesting to find that three types of particles coexisted: PS dark particles, PMMA lighter particles, and PS-1s/PMMA-1s composite particles. The composite particle morphology in Figure 5 indeed shows more clearly PMMA lighter region covering the PS dark phase, which should be compared to the composite particle morphology shown in Figure 4. This kind of composite particle morphology also corresponds well with the predicted morphology (case C with  $\theta = 153^\circ$ ) shown in Table V, using the equations listed in Table I. For the calculations, the volume ratio ( $V_r$ ) of the two polymer phases was kept constant ( $= 1$ ), and  $Y$ , the polymer phase–water interface area ratio of the original solvent-swollen polymer particle to final composite particle at 100% solvent removal, was equal to 249.93, and  $F$ , the polymer

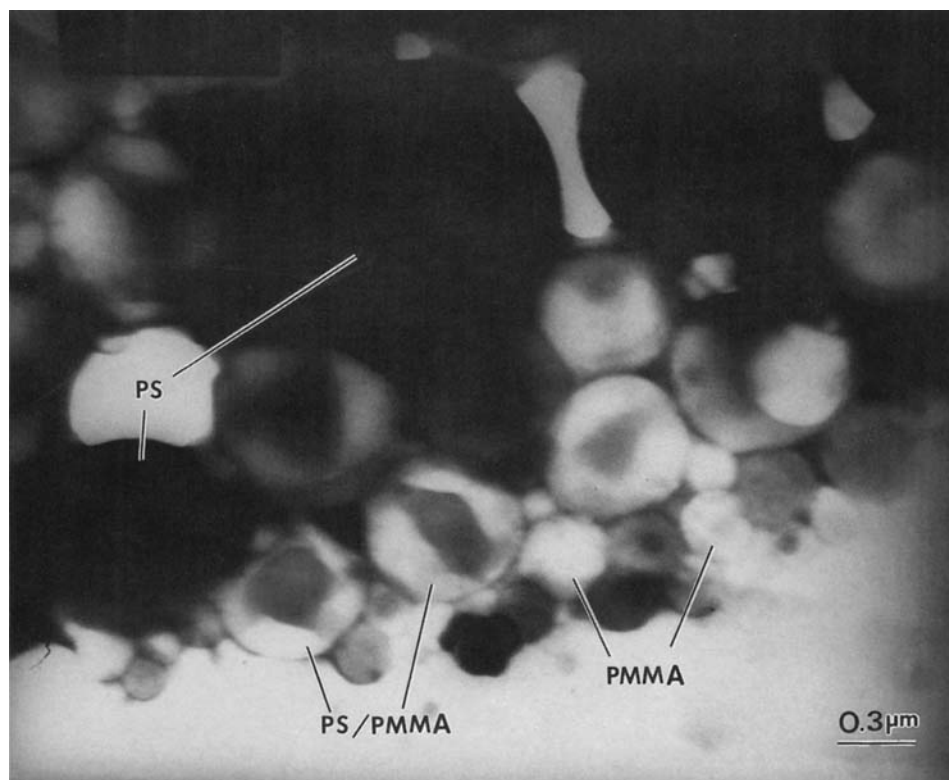


**Figure 5** TEM of PS-1s/PMMA-1s artificial composite latex particle morphology, at 0.6 g/cm<sup>3</sup> polymer concentration in toluene-swollen latex particles, after storing and tumbling for one week. Dark regions are polystyrene stained with RuO<sub>4</sub> and lighter regions are PMMA domains outlined using PTA stain.



**Table V Configuration of PS-1s/PMMA-1s System at 50/50 Polymer Weight Ratio, ( $\gamma_{1w} = 8.82$  dyn/cm,  $\gamma_{2w} = 8.23$  dyn/cm)**

Polymer Conc. (g/cm <sup>3</sup> )	$\gamma_{12}$ (dyn/cm)	Case Predicted
0.6	0.5	C, $\theta = 153^\circ$

phase-water interface area ratio of the overall composite particle (swollen with toluene at a polymer concentration of 0.6 g/cm<sup>3</sup>) to final composite particle was equal to 3.45. The corresponding interfacial tensions of polymers 1 and 2 in toluene against the aqueous phase were determined from Figure 2. The interfacial tension between polymer phases 1 and 2 in toluene was estimated from Figure 3 at 0.6 g/cm<sup>3</sup> polymer concentration.

It is possible that the pure PS and PMMA homopolymer latex particles observed in Figure 5 were generated during tumbling. In order to verify this

supposition, the composite latex at 0.6 g/cm<sup>3</sup> polymer concentration in the toluene-swollen latex particles was stirred by tumbling for one month at room temperature. The particle morphology is shown in Figure 6, where under direct irradiation in the TEM, only darker PS particles and lighter deformed PMMA particles were observed. This phenomena is also observed in the artificial composite latexes at lower polymer concentration, 0.35 g/cm<sup>3</sup>, and higher polymer concentration, 0.8 g/cm<sup>3</sup>, both are for toluene-swollen latex particles. Figures 7(a) and 7(b) show the particle morphology of the artificial composite latex at 0.35 g/cm<sup>3</sup> after one month of tumbling, and Figure 8 for the latex at 0.8 g/cm<sup>3</sup>. In both cases only PS particles (darker) and PMMA particles (lighter) can be observed in the micrographs. It seems that the change in viscosity of toluene-swollen latex particles and polymer-polymer interfacial tension by varying the toluene concentration in the particles in the range of polymer concentration from 0.35 to 0.8 g/cm<sup>3</sup> cannot avoid the formation of PS and PMMA individual polymer

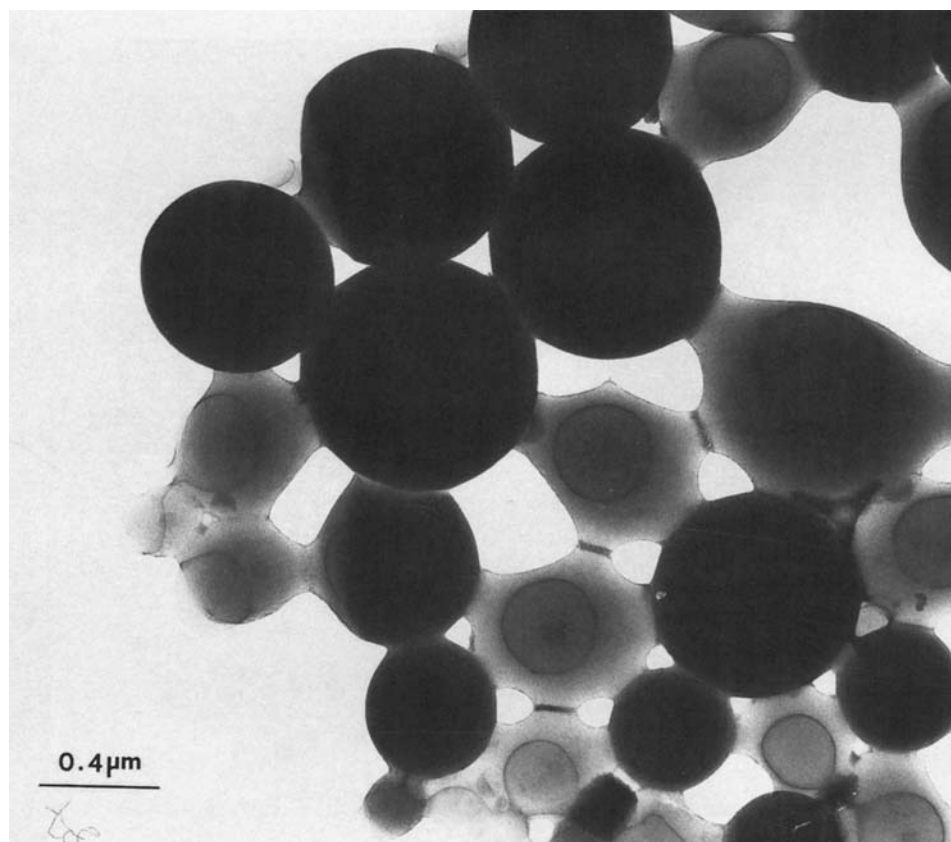


**Figure 6** TEM of particle morphology for PS-1s/PMMA-1s emulsion polymer system at 0.6 g/cm<sup>3</sup> polymer concentration in toluene-swollen latex particles after one month of storage and tumbling. Darker regions are PS particles. Lighter regions are PMMA particles.

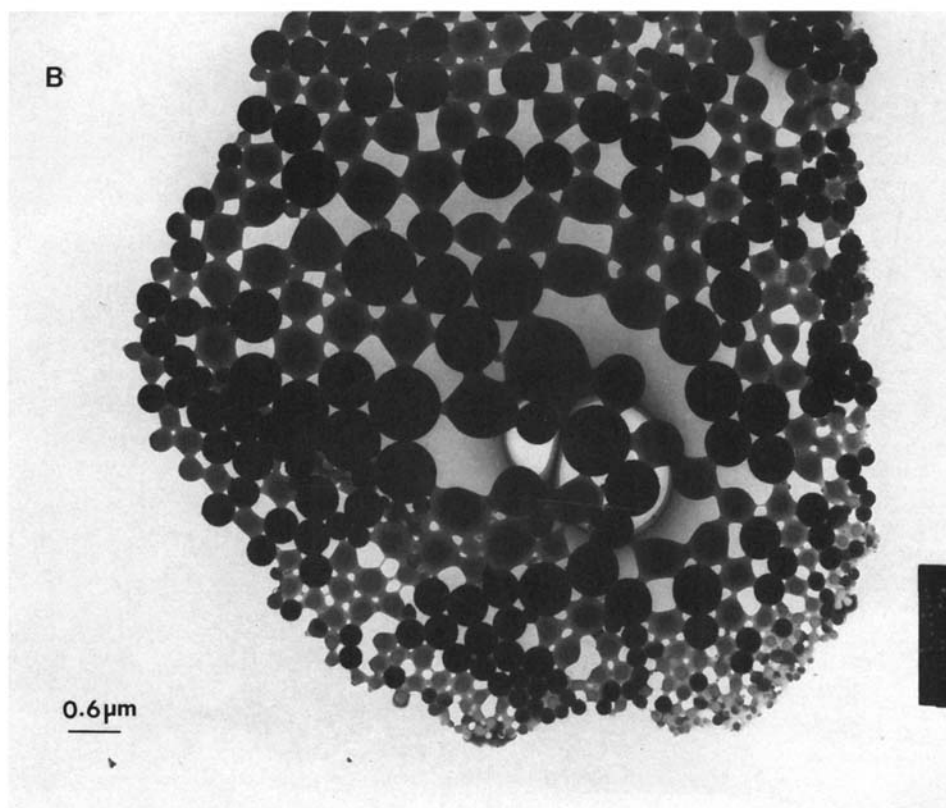
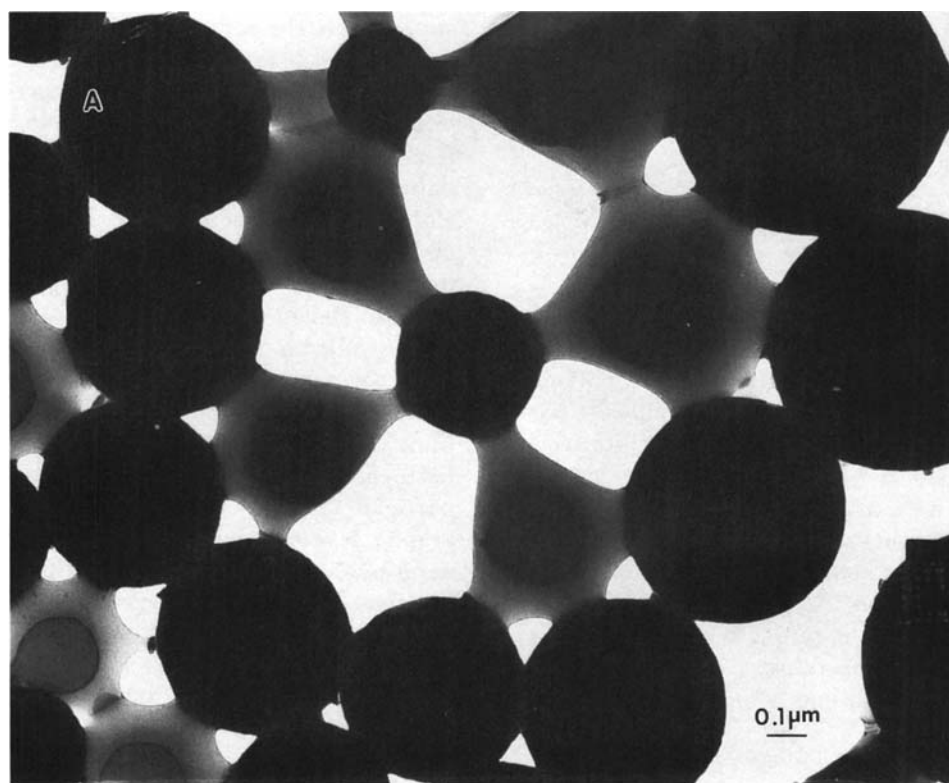


**Figure 7** TEM of particle morphology for PS-1s/PMMA-1s emulsion polymer system at  $0.35 \text{ g/cm}^3$  polymer concentration in toluene-swollen latex particles after one month of storage and tumbling. Darker regions are PS particles. Lighter regions are PMMA particles.

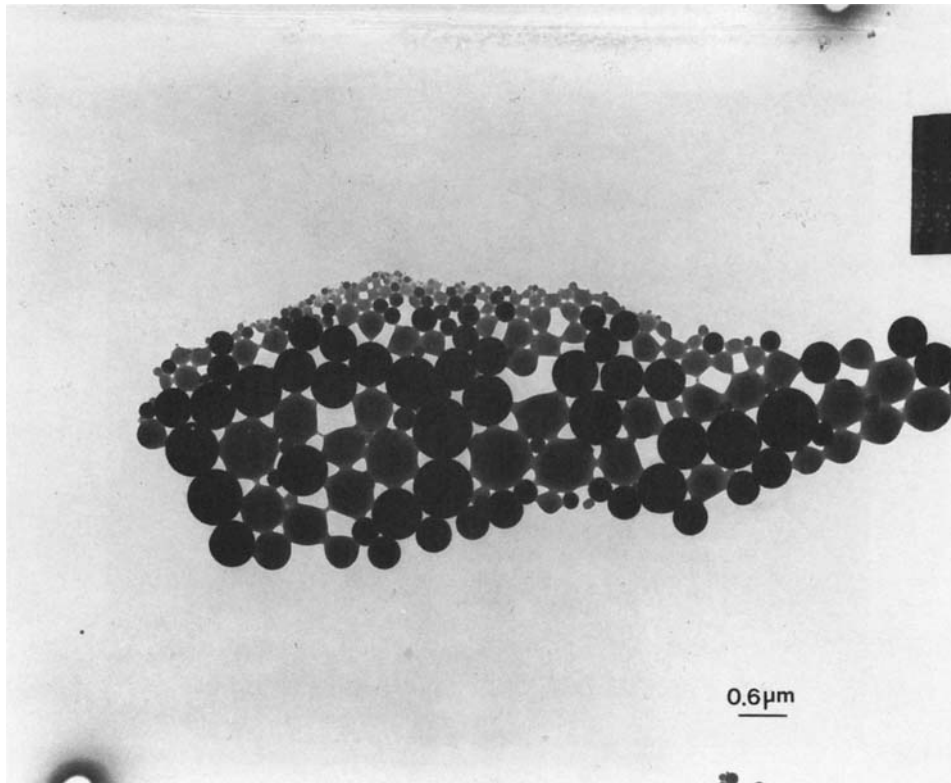


**Figure 8** TEM of particle morphology for PS-1s/PMMA-1s emulsion polymer system at  $0.8 \text{ g/cm}^3$  polymer concentration in toluene-swollen latex particles after one month of storage and tumbling. Darker regions are PS particles. Lighter regions are PMMA particles.

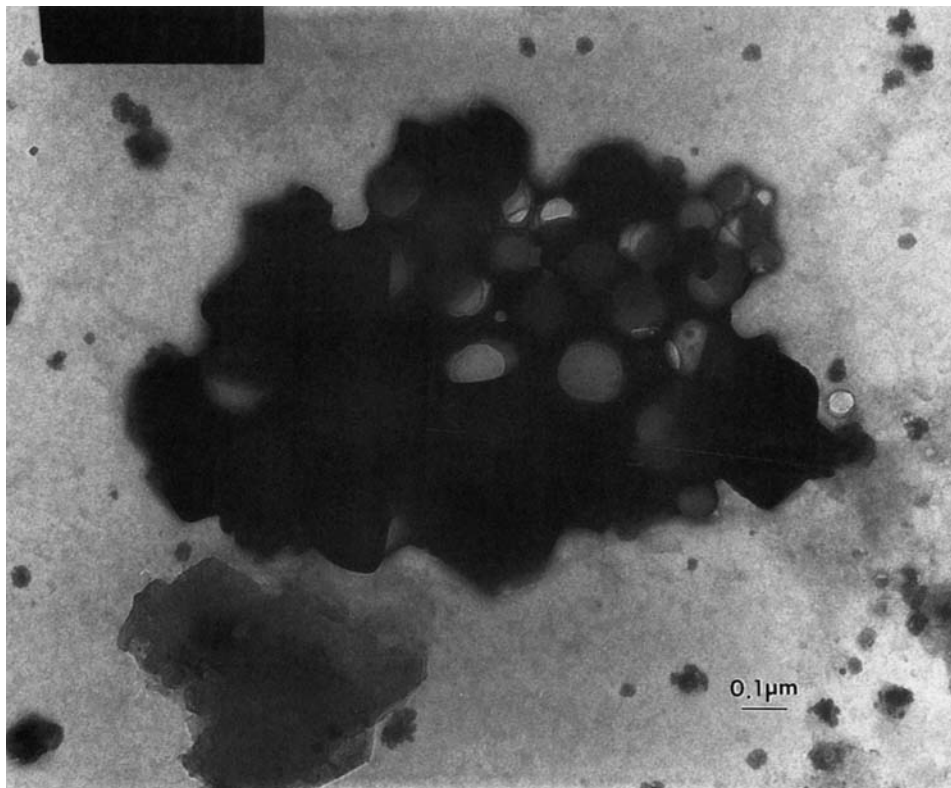


**Figure 9** TEM of Sample 1t of artificial composite latex of PS-2s/PMMA-2s after complete removal of toluene and tumbling 30 days. Darker regions are PS stained with  $\text{RuO}_4$  and lighter regions are PMMA domains outlined using PTA stain.

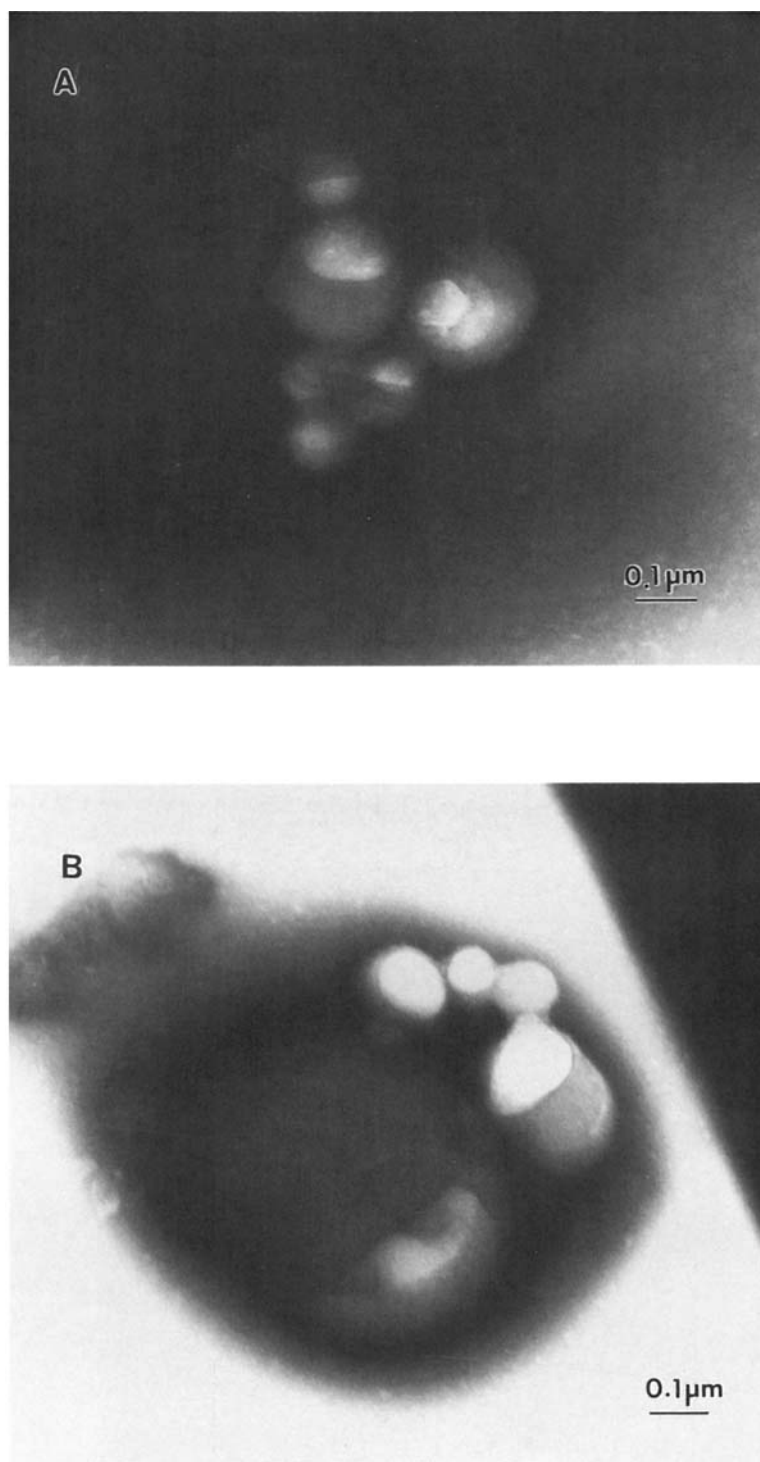


**Figure 10** TEM of sample 2 of artificial composite latex of PS-2s/PMMA-2s after re-swelling with toluene with 0.35 g/cm<sup>3</sup> polymer concentration and storing for 30 days. Darker regions are PS stained with RuO<sub>4</sub> and lighter regions are PMMA domains outlined using PTA stain.

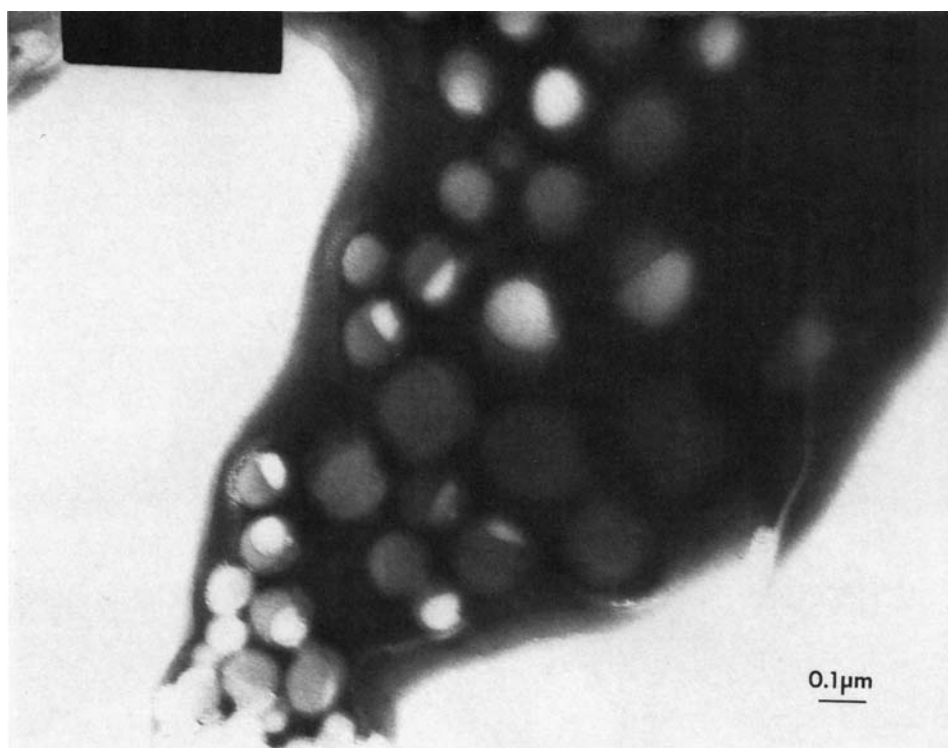


**Figure 11** TEM of sample 3 of artificial composite latex of PS-2s/PMMA-2s after re-swelling with cyclohexane with  $0.35 \text{ g/cm}^3$  polymer concentration and storing for 30 days. Darker regions are PS stained with  $\text{RuO}_4$  and lighter regions are PMMA domains outlined using PTA stain.

particles. The formation of PS and PMMA individual particles could be due to the shear forces introduced by tumbling and a “milling effect” due to the collision between polymer particles. The following experiments were conducted in order to verify this supposition.

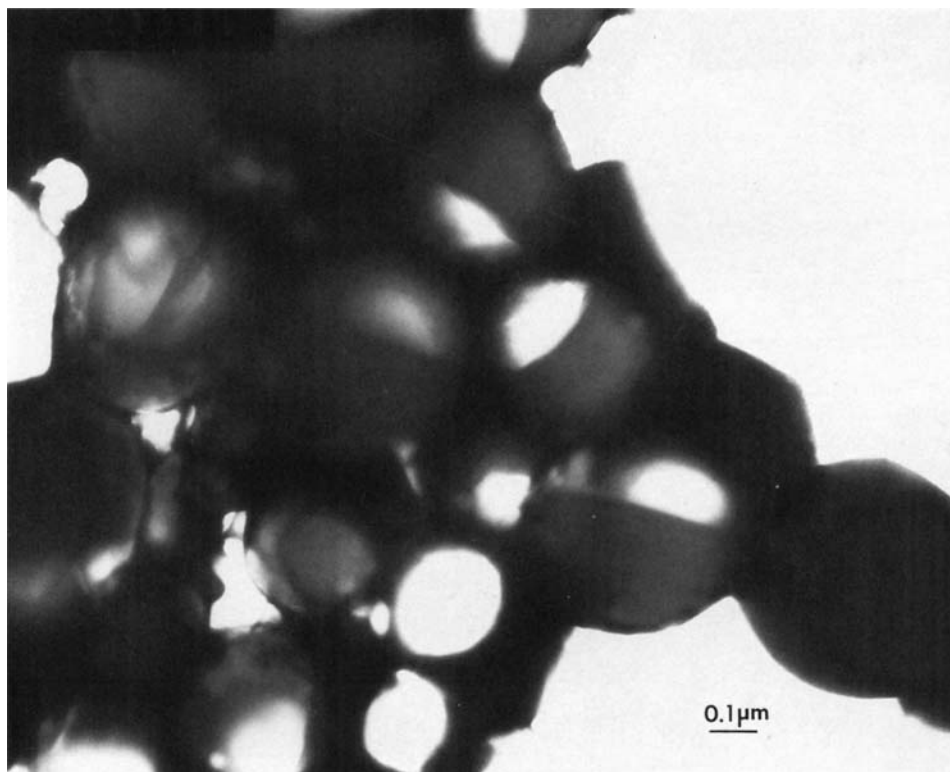
#### Morphology Observation for PS-2s/PMMA-2s Latex System

In order to examine the above phenomenon and the influence of shear forces on phase separation, morphological studies were conducted on an artificial composite latex PS-2s/PMMA-2s in which its component polymers were prepared by bulk solution polymerization at higher temperature ( $75^\circ\text{C}$ ), compared to PS-1s and PMMA-1s. The higher polymerization temperature resulted in lower molecular weights for PS-2s and PMMA-2s. It is expected that in the PS-2s/PMMA-2s composite particles, lower interfacial tension and thus higher degree of mixing should exist at the PS-2s and PMMA-2s interface than in the PS-1s/PMMA-1s composite particles. Therefore, it would be possible to prevent or retard

the formation of individual PS-2s and PMMA-2s particles during tumbling the PS-2s/PMMA-2s composite latex, if the formation of individual particles in the PS-1s/PMMA-1s system was due to shear forces.

Figure 9 shows the particle morphology of the artificial composite latex system PS-2s/PMMA-2s when the solvent was completely removed and followed by tumbling for 30 days (sample 1t). The PMMA domains (lighter region) can be seen to be encapsulated by PS (darker region) as expected from the lower interfacial tension of PS-2s compared to PMMA-2s (Fig. 2). This type of morphology confirms the formation of a composite latex particle after the process of particle preparation by direct emulsification.

Figure 10 shows the morphology of sample 2, the PS-2s/PMMA-2s latex particles re-swollen with toluene (polymer concentration =  $0.35 \text{ g/cm}^3$ ) and stored for 30 days, in which the PMMA (lighter region) is partially covered by PS (darker region). As expected, this type of encapsulation is due to the lower interfacial tension of the PS against the aqueous phase compared to that of the PMMA (see



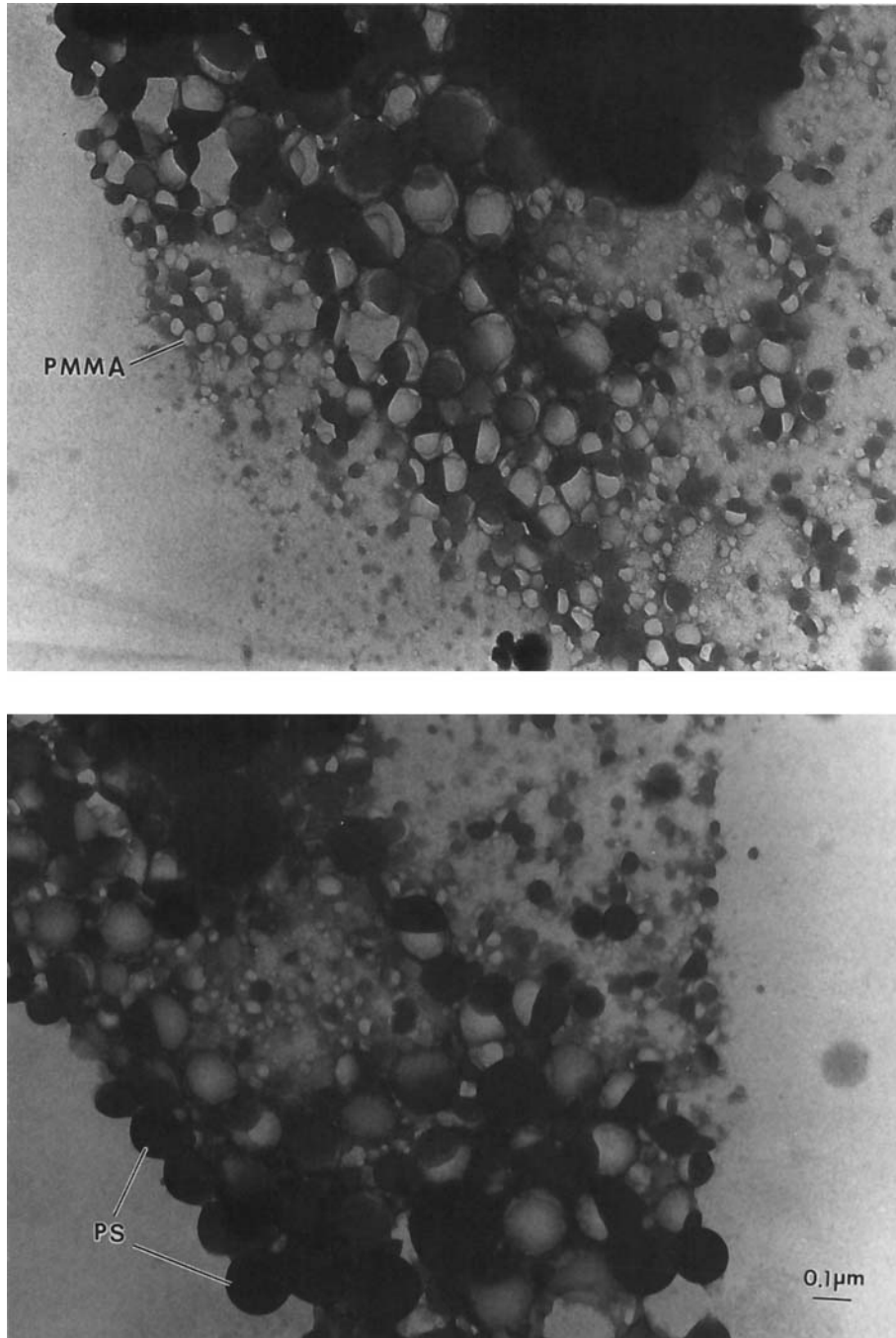
**Figure 12** TEM of sample 2t of artificial composite latex of PS-2s/PMMA-2s after re-swelling with toluene with  $0.35 \text{ g/cm}^3$  polymer concentration and tumbling for 30 days. Darker regions are PS stained with  $\text{RuO}_4$  and lighter regions are PMMA domains outlined using PTA stain.

Fig. 2). A similar morphology was also observed in sample 3 (see Fig. 11) where the particles were swollen by cyclohexane (polymer concentration =  $0.35 \text{ g/cm}^3$ ) instead of toluene. The observed morphology in both cases indicate that there are no individual PS or PMMA particles formed, due to the driving force of the lower interfacial tensions of the polymer phases.

Figure 12 shows the particle morphology of sample 2t, which was tumbled for 30 days after re-swelling with toluene (polymer concentration =  $0.35 \text{ g/cm}^3$ ). Interestingly, particles with a morphology similar to that of sample 2 (PMMA partially covered by PS) are still observed, instead of individual PS and PMMA particles shown in Figure 7 for the PS-1s/PMMA-1s system. This could be due to the lower molecular weights of the PS-2s and PMMA-2s polymers used in making the artificial composite latex compared to those of PS-1s and PMMA-1s polymers. Since the decrease in molecular weights of the two polymers is expected to result in a decrease of polymer phase 1/polymer phase 2 interfacial tension (see Fig. 3) and an increase in the thickness of the interfacial mixing zone.

Figure 13 shows the particle morphology of sample 3t, re-swollen with cyclohexane (polymer concentration =  $0.35 \text{ g/cm}^3$ ) and tumbled for one month. One can observe several individual PS (darker region) and a larger number of small PMMA (lighter region) particles coexisting with the composite particles, which display different shapes and sizes of the PMMA domains. This result could be attributed completely to the shear effects during tumbling. Although the use of cyclohexane as a swelling agent can also change the polymer interface properties, the particles still maintained the same type of morphology with the PMMA domains partially covered by the PS (see Fig. 11) as observed under conditions without tumbling. In addition, since the cyclohexane is a nonsolvent for the PMMA, the PS domains in the composite particles should contain a higher concentration of cyclohexane, which should lower its viscosity compared to the PMMA domains. Therefore, under the shear forces of tumbling and milling effect due to the collision between particles, phase separation of the two polymers in such particles would increase.

Based on the above study, one can conclude that



**Figure 13** TEM of sample 3t of artificial composite latex of PS-2s/PMMA-2s after re-swelling with cyclohexane with  $0.35 \text{ g/cm}^3$  polymer concentration and tumbling for 30 days. Darker regions are PS stained with  $\text{RuO}_4$  and lighter regions are PMMA domains outlined using PTA stain.

the formation of PS and PMMA individual particles is mainly due to the shear forces and milling action encountered during tumbling of the artificial composite particles swollen with solvent. In the course of the preparation of composite particles by seeded

emulsion polymerization, agitation is usually supplied, which can induce similar shear force and collision between particles. Therefore, it is expected that the degree of phase separation between polymers in composite particles could also be affected

by agitation, depending on the viscosity of polymer phases, the interfacial tension, and the degree of mixing at the two polymer interface.

## CONCLUSIONS

Two artificial composite latexes, PS-1s/PMMA-1s and PS-2s/PMMA-2s, were prepared using direct emulsification of corresponding polymers in toluene solution. The PS-2s/PMMA-2s composite latex containing lower molecular weights of PS and PMMA polymers showed the opposite type of encapsulation to the PS-1s/PMMA-1s latex particles containing higher molecular weights of polymers. The morphology of these artificial composite latexes after their preparation correspond well with the predicted morphology based on thermodynamic analysis. However, upon tumbling the toluene-swollen composite latex particles for a period of time, the PS-1s/PMMA-1s latex resulted in the formation of individual PS and PMMA particles, whereas the PS-2s/PMMA-2s latex did not. After removing all the toluene from the PS-2s/PMMA-2s composite latex particles, they were reswollen with cyclohexane and tumbled for 30 days. Several individual PS and PMMA particles were observed to coexist with composite particles that display different shapes and sizes of PMMA domains. These results indicate that the formation of PS and PMMA individual particles is mainly due to shear forces and milling action encountered during tumbling of the artificial composite particles swollen with solvent. The degree of phase separation between polymers in composite particles could be affected by agitation, depending on the viscosity of the polymer phases and the interfacial tension or degree of mixing at the interface between the two polymers.

## REFERENCES

1. Y. C. Chen, V. L. Dimonie, and M. S. El-Aasser, *J. Appl. Polym. Sci.*, **42**, 1049 (1991).
2. Y. C. Chen, V. L. Dimonie, and M. S. El-Aasser, *Macromolecules*, **24**, 3779 (1991).
3. V. L. Dimonie, M. S. El-Aasser, and J. W. Vanderhoff, *Polym. Mat. Sci. Engr.*, **58**, 821 (1988).
4. M. Okubo, Y. Katsuta, and T. Matsumoto, *J. Polym. Sci. Polym. Lett. Ed.*, **18**, 481 (1980).
5. S. Lee and A. Rudin, *Makromol. Chem., Rapid Commun.*, **10**, 655 (1989).
6. M. S. El-Aasser, Latex Preparation by Direct Mini-emulsification of Polymer Solutions and Polymerization of Monomer Miniemulsions, 22th Annual Short Course-Advances in Emulsion Polymerization and Latex Technology, Volume III, Lehigh University, June 1991.
7. J. W. Vanderhoff, M. S. El-Aasser, and J. Ugelstad, U.S. Pat. 4,177,177 (1979).
8. S. Torza and S. Mason, *J. Colloid Interface Sci.*, **33**, 67 (1970).
9. D. Sundberg, A. P. Casassa, J. Pantazopoulos, and M. R. Muscato, *J. Appl. Polym. Sci.*, **41**, 1429 (1990).
10. Y. C. Chen, V. L. Dimonie, and M. S. El-Aasser, *J. Appl. Polym. Sci.*, to appear.
11. M. Kurata, M. Iwawa, and K. Kamada, "Viscosity-Molecular Weight Relationships and Unperturbed Dimensions of Linear Chain Molecules," in J. Brandrup and E. H. Immergut, Eds., with the collaboration of H.-G. Elias, *Polymer Handbook*, Wiley-Interscience, New York, 1966, pp. IV-1-IV-72.
12. O. Shaffer, M. S. El-Aasser, and J. W. Vanderhoff, *Proceedings of 41st Ann. Mtg. Electro Microscopy Soc. Am.*, San Francisco Press, San Francisco, 1983, p. 30.
13. J. L. Lando and H. T. Oakley, *J. Colloid Interface Sci.*, **25**, 526 (1967).
14. Y. C. Chen, Ph.D. Dissertation, Lehigh University (1991).
15. D. Broseta and L. Leibler, *J. Chem. Phys.*, **87**, 7248 (1987).

Received October 16, 1991

Accepted December 19, 1991